Journal of Loss Prevention in the Process Industries 43 (2016) 688–699

Contents lists available at ScienceDirect

Journal of Loss Prevention in the Process Industries

journal homepage: www.elsevier.com/locate/jlp

Experimental data and CFD performance for CO_2 cloud dispersion analysis

A.M. Schleder, M.R. Martins*

Analysis, Evaluation and Risk Management Laboratory (LabRisco), Naval Architecture and Ocean Engineering Department, University of Sao Paulo, Av. Prof. Mello Moraes, 2231, 05538-030 Sao Paulo, Brazil

ARTICLE INFO

Article history:
Received 2 February 2016
Received in revised form
22 March 2016
Accepted 24 March 2016
Available online 31 March 2016

Keywords:
Consequence analysis
Carbon dioxide dispersion
Dispersion field tests
Computational fluid dynamics
FLACS software

ABSTRACT

Dispersion of hazardous gas releases represents a major threat to health and to the environment; therefore, the prediction of the dispersion features raises great interest. In recent years, with the increase in computational capacity, the interest in Computational Fluid Dynamics (CFD) tools to evaluate dispersion analysis has increased. With the growing use of CFD tools to perform dispersion analysis in different scenarios, it is imperative to amplify the availability of experimental data in order to allow validations studies to contribute to understanding the real capacity of CFD tools to properly represent real cases. The second stage of the field tests conducted by a joint venture between the University of São Paulo and the Universitat Politecnica de Catalunya was established to investigate the performance of CFD tools when analyzing cloud dispersion of hazardous substances by means of ad-hoc experimentation. The experiments consisted of CO_2 clouds formation and dispersion tracking of releases of up to 0.85 kg s^{-1} of about 40 s of duration in a 600-m^2discharge area. We provide a description of the tests and the main results of the simulation using the FLACS software; the peak concentrations for 51 sensors placed at the dispersion cloud path are provided here and compared with CFD simulations. In general terms, the CFD simulator presented good performance; all the statistical performance measures were well within the acceptable range. However, the simulator performance presented sensitivity to the wind profile, especially when cross wind occurs.

1. Introduction

The industrial and technological development of the current society increases the number of activities involving toxic and flammable substances. Dispersion of hazardous gas releases occurring in transportation or storage installations represent a major threat to health and to the environment. Therefore, the prediction of the dispersion features is highly relevant to define the extent and the nature of the effects caused by such releases and thus to quantify the possible damage, safety areas and control options to mitigate the impact.

In recent years, with the increase in computational capacity, the interest in Computational Fluid Dynamics (CFD) tools to evaluate dispersion analysis has risen due to the current requirements for risk analysis of accidental releases of hazardous substances (e.g. Sklavounos and Rigas, 2006; Cormier et al., 2009; Tauseef et al., 2011). Although CFD tools take significantly longer to perform dispersion analysis than the traditional empirical and integral models, they allow taking into account the geometry of elements present in real scenarios, such as barriers or semi-confined spaces.

The CFD tools have been proven promising to perform dispersion analyses; however, they still present some challenges to overcome. In CFD simulations, several computational parameters must be set by the analyst and the decisions taken about them may significantly affect the results; for example, in a typical simulation, the analyst needs to select the variables of interest, to define the computational domain, to select a turbulence model from a set of available options, to specify the method of discretization and the boundary conditions, among other parameters. Consequently, as reported by Plasmans et al. (2012), the results from CFD simulations may present great variability when different tools are used and/or different CFD analysts evaluate the simulations.

In order to treat this issue, many authors have conducted sensitivity analyses (Cormier et al., 2009; Pandya et al., 2012; Gant et al., 2013; Schleder et al., 2014a) and validation studies to provide insights on how to appropriately set CFD simulations; however, even

* Corresponding author.
E-mail address: mrmartin@usp.br (M.R. Martins).

http://dx.doi.org/10.1016/j.jlp.2016.03.027
0950-4230/

recent studies have to make use of experimental data of tests performed decades ago due to the absolute absence of public data about recent dispersion experiments. Hanna et al. (2004) and Mazzoldi et al. (2008) made their assessment using the experimental data of two very traditional tests, the Prairie Grass and Kit Fox evaluated in 1956 and 1995, respectively. Hanna et al. (2004) also use the MUST and EMU-L series, windtunnel tests evaluated in 2001 and 1997. In a very recent paper, Albani et al. (2015) use Prairie-Grass, the Hanford and the Copenhagen tests data performed in 1956, 1985 and 1981, respectively. Kumar et al. (2015) present a validation study based on experimental data of the MUST tests undertaken in 2001. We evaluated a sensitivity analysis using the field tests performed by the Health and Safety Laboratory (HSL) at the HSL laboratories in Buxton, England in 2001 (Schleder et al., 2014a,b).

Liu et al. (2015) presents a rich literature review focused on CO_2 dispersion in which the authors show that there are only a few field tests and most are focused on the decompression of CO_2 during the release and not on the dispersion per se; in their validation study, they compare the simulation results with the experimental data of the tests evaluated in Thorney Island in 1985.

Field experiments dealing with dispersion are sparse in the literature and experiments dealing with dispersion in complex environments, with some degree of obstruction are really rare. The majority of these tests publicly available in the literature were undertaken decades ago, and the data generated are not comprehensive enough for an exhaustive evaluation of CFD tools performance; moreover, many of those present only values of peak concentrations in arcs around the release source, not allowing a comprehensive understanding of the dispersion features.

With the increasing use of CFD tools to perform dispersion analysis in different scenarios, it is imperative to amplify the availability of experimental data in order to allow validation studies to contribute to understanding the real capacity of CFD tools to properly represent real cases.

Aiming to overcome this drawback, a joint venture between the University of São Paulo (USP) and the Universitat Politecnica de Catalunya (UPC) was established to investigate the performance of CFD tools when analyzing cloud dispersion of flammable/toxic substances by means of ad-hoc experimentation.

The first stage of the experiments planned in this project was undertaken at Can Padró Security and Safety training site between 22nd and 25th July 2014 and consisted of LPG cloud formation and dispersion tracking as reported by Schleder et al. (2015).

A second stage of experiments was performed at the Sports Center of the University of São Paulo (CEPEUSP) between 11th and 14th August 2015 and consisted of CO_2 cloud formation and dispersion tracking. A description of this stage presents the main results of the simulation using FLACS software, which is a CFD tool specifically developed for consequence analysis. The aims of this paper are to provide new sets of experimental cloud dispersion data, particularly for those problems involving dispersion scenarios with barriers to the international community and to present the main results of CFD performance simulating the field test.

2. Experimental setup

The field tests involved continuous releases of CO_2 in the atmosphere with consequent cloud formation. Preliminary tests and ten trials more were performed totaling about 200 kg of CO_2 released during the tests. The cloud dispersion was intensively monitored to determine the evolution of the concentration in time and space.

The CO_2 was stored in pressurized cylinders (around 120×10^3 hPa at ambient temperature) located roughly 3 m apart from the release point. The CO_2 flowed through a 38 mm diameter pipe with a total length of 2 m up to the release point, which was located at a 1 m height (Fig. 1).

Pressure and temperature were measured at the release point by an electronic pressure transmitter (Barksdale, type UPA5) and one K-type thermocouple located 0.05 m upstream of the outlet orifice, both recording at a frequency of 4 Hz. Thus, the mass flow rate ant the jet velocity at the outlet orifice was calculated assuming isentropic expansion between the stagnation point and the orifice jet exit by applying the appropriate thermodynamic relationships. The total amount of gas released was obtained by the integral of the mass flow rate variation during the release and verified by weighing the cylinders used in the tests.

In order to monitor the cloud concentration, sensors were arranged over a 200 m^2 area (20 m in the release direction and 10 m in cross direction). 51 self-powered electrochemical oxygen sensors (2FO flue gas sensor of CiTicel) were placed at 17 different locations within the discharge area at three different heights: 0.1, 0.6 and 1.2 m (as presented in Fig. 2). These sensors provide an indirect measure of CO_2 concentration assuming that any decrease in the concentration of oxygen was caused by displacement of oxygen by the CO_2 vapor. The sensors were made of a galvanic cell, being the current flow between the cell electrodes proportional to the oxygen concentration to be measured. A small amount of oxygen is consumed in the cell reaction in order to produce the current flow. Additionally, the sensors had a bridge resistor to provide voltage power (mV) as output. Assuming an atmospheric oxygen concentration of 20.9% (volume) and an atmospheric nitrogen concentration of 79.1%, the CO_2 vapor concentration $[CO_{2v}]$ can then be expressed as:

$$[CO_{2v}] = 1 - [O_2] - \frac{79.1[O_2]}{20.9} \quad (1)$$

Being $[O_2]$ the oxygen concentration detected by the sensors.

Note that CO_2 is an acid gas; therefore, it will be slightly absorbed by the electrolyte and tends to increase the flux of oxygen to the electrode. This gives an enhanced oxygen signal of about 0.3% per 1.0% CO_2; thus, the CO_2 vapor concentration $[CO_{2v}]$ was corrected by this rate (City Technology Limited, 2010).

The experiments were designed to investigate the influence of barriers placed in the dispersion route; thus, five different layouts were used during the tests: i) without barriers, dispersion with no obstacles; ii) a 1-m high and 1-m wide fence placed 9 m from the release point; iii) a 1-m high and 2-m wide fence placed 9 m from the release point; iv) a fence in L format (1 m × 1 m) placed 9 m from the release point; v) a fence in L format (1 m × 1 m) placed 9 m from the release point in an inverse position of the previous layout. The different types of fences used during the tests are represented in Fig. 3.

Moreover, 4 ultrasonic wind sensors (WindSonic OP1 of Gill Instruments) and 1 meteorological station (Vantage Vue Wireless of Davis Instruments) were used to monitor the weather conditions. Wind direction and speed measurements were recorded at a frequency of 1 Hz; the wind sensors were placed at 1 m and 2 m in height at positions W1AB and W2AB (see Fig. 2). Ambient temperature and relative humidity were obtained by the meteorological station. The use of a specific weather station at the site of experiments was important since the nearest national weather station is located in a more sheltered area with slightly lower temperatures; and the coverage area informed by the weather station operators does not include the tests site.

Finally, to register and to store the sensors data, two data acquisition systems (model ADS2002IP-B-5 of Lynx Electronic Technology) were used. The data were recorded at a rate of 4 Hz Fig. 4 shows an overview of the experimental arrangement.

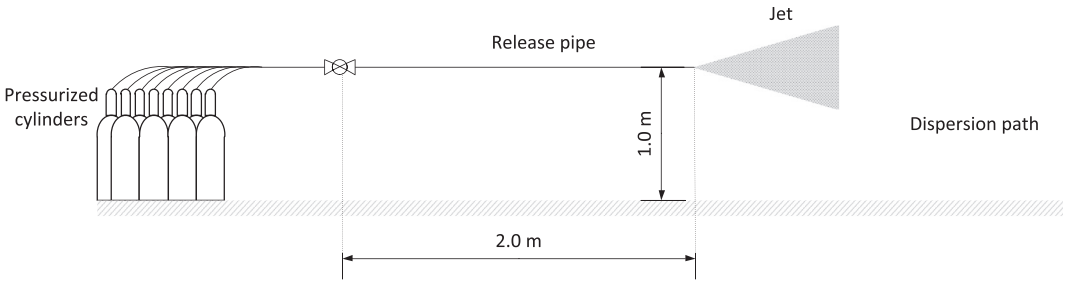

Fig. 1. Layout of experimental installation.

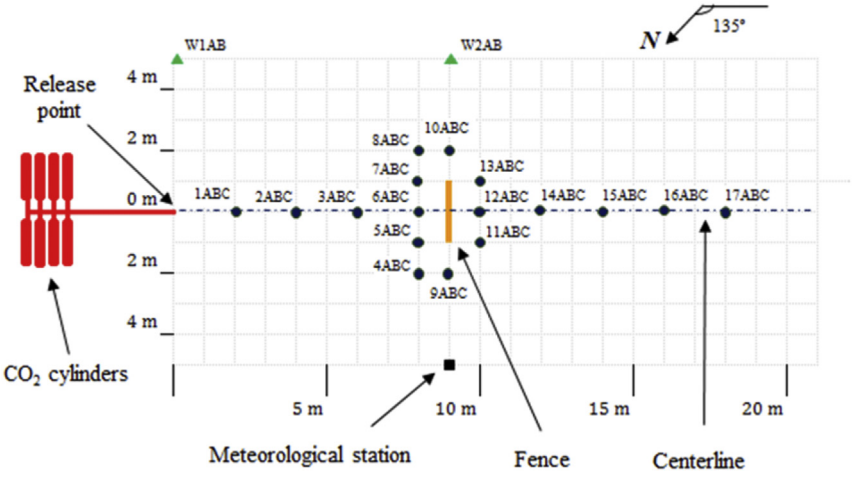

Fig. 2. Sensor array (blue circles); the numbers are identifiers of the masts to which the sensors were attached and letters A, B and C represent the sensors height, at 0.1 m, 0.6 m and 1.3 m, respectively. (e.g. the mast "3ABC", located on the centerline of the dispersion path 6 m apart from the release point, sustained sensors at three heights: 0.1 m, 0.6 m and 1.2 m). The green triangles named W1 and W2, represent the location of the anemometers at 1-m height (A) and 2-m height (B). (For interpretation of the references to color in this figure legend, the reader is referred to the web version of this article.)

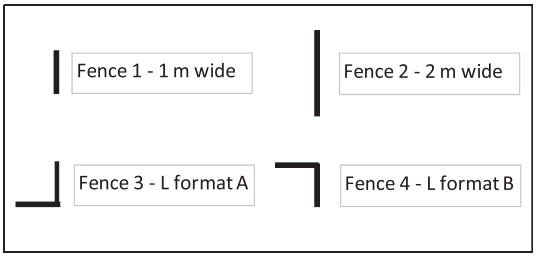

Fig. 3. Fences used during the field tests.

Fig. 4. Photo of the experimental arrangement; the release point, the masts and the fence.

3. CFD modeling

CFD simulations were performed in order to compare the simulation results with the experimental data. The FLACS® software (GexCon AS, 2013a) was used to evaluate the simulations; FLACS is a CFD tool developed especially for consequence modeling. It uses conservation equations for mass, energy, and momentum; it solves Reynolds Averaged Navier-Stokes (RANS) equations based on the k-ε turbulence model of Launder and Spalding (1974). HSE (2013) reports that the RANS approach is extensively accepted in CFD studies for dispersion analysis; it is grounded on the idea of separating the fluid velocity components and scalar quantities (such as pressure, temperature, concentration) into mean and fluctuating components, then transport equations are used to evaluate the model. Concerning the turbulence model, the Launder & Spalding model (1974) treats the turbulent kinetic energy and its dissipation rate; transport equations are used to calculate the magnitudes of these two variables simultaneously with the evolution of the equations that governs the mean flow behavior.

3.1. Description of scenario conditions

The scenario conditions cover both initial conditions and boundary conditions of the domain; the values used to perform the simulations of each trial performed are presented in Table 1. Values

of wind direction and speed, ambient temperature, ambient pressure and relative humidity were considered as the median of the values recorded along each test.

The ground roughness was assumed to be equal to 0.03, which is the characteristic value for concrete surfaces (GexCon AS, 2013b). The Pasquill class used was D – slightly stable for trials 1–7 although the cloud cover and wind speed indicated class B; this was necessary because the current version of FLACS may become unstable to model an unstable atmosphere condition (this problem was previously reported by Hansen, 2010). For trials 8–10, the Pasquill class E – stable was simulated.

The minimum and the maximum values (registered along the trials) of the pressure and temperature in the outlet orifice are also detailed in Table 1. 1s averages of the measured temperature and pressure values were used to calculate the release rate. As previously mentioned, the jet velocity in the outlet orifice and the mass flow rate were calculated assuming isentropic expansion between the stagnation point and the orifice jet exit; the total amount of fuel released was obtained by the integral of the mass flow rate during the release. During the simulations, a 1-s-averaged variable mass flow rate was considered.

3.2. Domain and grid definition

The simulation domain was built using a single block Cartesian grid considering the FLACS user manual guideline recommendations (GexCon AS, 2013b). An orthogonal base X, Y and Z was used, being X horizontal and parallel to the jet direction, Y horizontal and perpendicular to the jet direction and Z, vertical. The domain extended 55 m in the X direction (from 5 m before the release point to 50 m after the release point), 30 m in the Y direction (centered on the release point) and 10 m in the Z direction (from de ground level). As such, the release point coordinate was (0, 0, 1.0) in the domain. The domain was defined using two types of meshes (Fig. 5): the former being a coarse (macro) grid, representing the zone where the dispersion is expected to occur; and the latter being a refined (micro) grid, representing two different swaths intersecting around the release point: one vertical, formed by a mesh of cells on the centerline of the dispersion path, and the other horizontal, formed by a mesh of cells centered at the release point and 1.0-m height (i.e. release height).

The cells were represented by 1 m edge cubes at the macro grid. In order to set the micro grid, the FLACS guidelines (GexCon AS, 2013a,b) were followed; they specify that the area of the expanded jet (A_{jet}) must be solved in only one cell and that the area of this cell across the jet (A_{cv}) should be larger than the area of the expanded jet but not larger than twice A_{jet}. The expected jet area after the expansion at ambient pressure was estimated using the FLACS jet utility –which is based on a one-dimensional model for the release of an ideal gas from a pressurized reservoir through a nozzle in an open atmosphere (GexCon AS, 2013b) – and the dimensions of the cell across the jet were defined so that the area fell between the specified limits. Thus, the width and height of the micro grid cells were fixed at 0.06 m (as a function of the jet area expected after the expansion at ambient pressure).

The FLACS guidelines also recommend that the aspect ratio (the ratio between the smallest and largest side of the cell) of the micro grid has to be no larger than five (due to the stability of the numerical solution); thus, the length of the cells was fixed at 0.30 m. Next, the cells near the leak were smoothly increased to the macro grid resolution maintaining the maximum change in grid resolution from one grid cell to the next one at less than 40% (as recommended by the FLACS guidelines).

Finally, monitoring points were inserted in the simulation specifications at the same locations where the sensors were placed in the field, which allowed the measured values of concentration to be compared with the simulated values.

4. Results and discussion

As previously stated, one objective of this study is to offer new sets of experimental cloud dispersion data, particularly for those problems involving dispersion scenarios with obstacles, to the international community interested in model validation studies and in new insights about gas dispersion in environments with barriers. The most relevant data acquired during the experiments are discussed in this section and more detailed information is included in Annex A (i.e. CO_2 release rates and peak concentrations).

The second aim of this paper is to present the main results of CFD performance reproducing cloud dispersion in scenarios with obstacles. To address this objective, concentration was defined as the main variable of interest. The model performance was verified using typical statistical performance measures of the approach summarized by Chang and Hanna (2004); these include the fraction of predictions within a factor of two of observations (FAC2), the fractional bias (FB), the geometric mean bias (MG), the normalized mean square error (NMSE) and the geometric variance (VG). These key indicators are defined as follows:

$$FAC2 = \text{fraction of data that satisfy } 0.5 \leq \frac{C_p}{C_o} \leq 2.0 \tag{2}$$

$$FB = \frac{\left(\overline{C_o} - \overline{C_p}\right)}{0.5\left(\overline{C_o} + \overline{C_p}\right)} \tag{3}$$

Table 1
Scenario conditions.

Variable	Unit	P1	P2	P3	P4	P5	P6	P7	P8	P9	P10
Ambient Temperature	°C	21.5	21.5	23.8	23.8	24.3	24.3	21.1	21.1	19.1	19.1
Ambient pressure	hPa	933	933	933	933	930	930	930	930	931	931
Relativity humidity	%	52	52	44	44	54	54	78	78	80	80
Wind direction (wind from north to south equal to 0°)	°	0	186	141	124	259	249	231	191	206	227
Wind speed at 1-m height	m s^{-1}	0.6	0.4	0.8	0.8	0.3	0.8	1.3	1.1	1.2	0.9
Release duration	s	41	39	39	40	32	32	32	39	42	43
Pressure release range (min/max)	hPa	32	17	134	14	143	372	41	95	49	2
		1260	1248	2800	791	1197	916	695	541	1215	688
Amount of fuel released	kg	16.82	18.98	28.05	16.33	16.90	15.76	12.97	13.08	22.16	15.76
Discharge rate (min/max)	Kg s^{-1}	0.04	0.07	0.09	0.08	0.2	0.38	0.13	0.20	0.14	0.01
		0.54	0.65	0.84	0.56	0.63	0.58	0.52	0.46	0.63	0.51
Fence (as in Fig. 3)	–	2	1	–	3	3	4	3	4	2	–

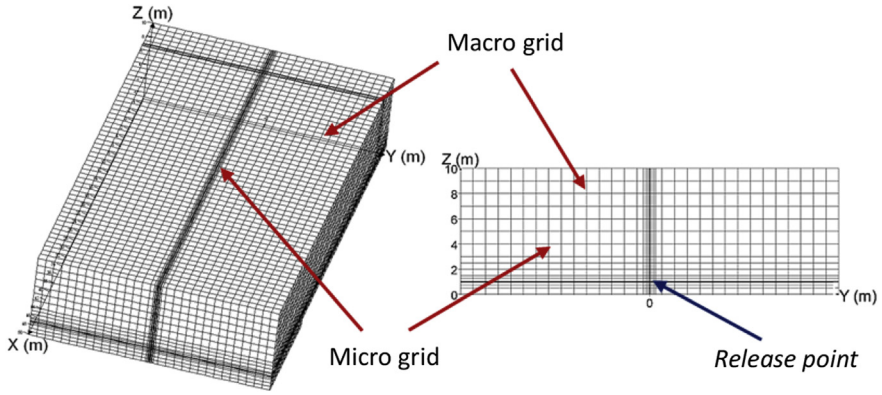

Fig. 5. Grid representation; the darkest areas representing the micro grid and the clearest areas representing the macro grid.

$$MG = \exp\left(\overline{lnC_o} - \overline{lnC_p}\right) \quad (4)$$

$$NMSE = \frac{\overline{(C_o - C_p)^2}}{\overline{C_o}\,\overline{C_p}} \quad (5)$$

$$VG = \exp\left[\overline{(lnC_o - lnC_p)^2}\right] \quad (6)$$

where:

C_o: observed concentrations
C_p: predicted concentrations
overbar ($\overline{C}$): average over the dataset

These indicators were widely used for CFD validation purposes; they were recommended by Weil et al. (1992) and Hanna et al. (2004) to evaluate air quality models. Later on, they were recommended by HSE in the Model Evaluation Protocol (Ivings et al., 2007) and more recently they were used by several authors (Mazzoldi et al., 2008; Coldrick et al., 2009; Ivings et al., 2013; Xing et al., 2014; Schleder et al., 2015).

There is not a single best measure and it is necessary to use a set of indicators to asses a model; as presented by Chang and Hanna (2004), the factor of two (FAC2) range, which analyses whether the simulated values fall within a ± factor of two of the measured data is the most robust indicator.

It must also be noted that for dispersion modeling, MG and VG are better indicators than FB and NMSE, since the concentrations usually vary by several orders of magnitude and the FB and NMSE are very sensitive to extreme high and low concentrations, even infrequent. The MG and VG provide a more well-adjusted treatment, since the logarithmic measures are less sensitive to the extremes.

As defined in Chang and Hanna (2004), the dispersion model is defined as acceptable if at least 50% of the predicted points fall within the factor 2 range from observations ($0.5 < FAC2 < 2.0$), the random scatter is about two or three of the mean ($VG < 4$ or $MNSE < 9$) and the relative mean bias within ±30% ($0.7 < MG < 1.3$ or $-0.3 < FB < 0.3$).

The measure indicators above are defined by a dataset formed by pairs of C_o and C_p; for dispersions models, the pairing assessment can be made in three ways: pairing in time only (i.e. maximum concentration at a specific moment anywhere in the domain), pairing in space only (i.e. maximum concentration in a specific space) and pairing in time and space. Commonly, for dispersion models, these indicators are presented in terms of maximum concentrations measures in concentric arcs at different distances from de release point (Hanna et al., 2004; Mazzoldi et al., 2008); this approach disregards the effects of the wind direction, comparing only the magnitude of peak concentrations in an arc apart from the release point. We performed the pairing in space for each monitor point presented in Fig. 2; therefore, the effects of wind direction were taken into account and the analysis of the statistical performance measures was more rigorous than the usual approach.

It is also worth noting that both MG and VG are extremely sensitive for low values; thus, they were calculated considering a minimum threshold equal to 0.1% (only points where the predicted peak concentration was higher than 0.1% [vol] were considered). The assumption of a minimum threshold is recommended by Chang and Hanna (2004) and later applied by Xing et al. (2014) in their CFD validation study.

Table 2 presents the performance measures concerning peak concentrations at each monitored point of the different trials: the percentage of predicted values within the FAC2 range for each trial, the FB and NMSE, the VG and MG considering the minimum threshold and, finally, the maximum concentration difference, the maximum difference found between the measured and predicted value among all the monitored points (i.e. on trial P1, the maximum difference values equals 0.8%, because the peak concentration measured for the point with the greatest discrepancy equals 1.60% and the peak concentration predicted equals 0.76%).

In general terms, the model presents good statistical indicators: over 70% of the predicted values for peak concentrations fall within the FAC2 range; FB and MG show that the simulator presents a slight under prediction between 10% and 20% (averaged FB and MG); the VG indicates that the random scatter is about a factor of two of the mean; and finally, although the NMSE presents values very close to the ideal (equal to zero), the value should be seen with caution because of compensating errors (one more reason to prefer the use of MG and VG over FB and NMSE).

By examining the statistical performance measures of each trial, trials P1 and P2 are verified to present performance measures very close to ideal values; about 90% of the predicted peak concentrations fall within the FAC2 range as shown in Figs. 6 and 7 (they show experimental versus simulated values of peak concentrations calculated from 51 concentration sensors at the dispersion area along the tests – FAC2 confidence limits are included in the figures below as dashed red lines, 90% of the plotted points fit within this range).

Simulations of trials P3 and P4 did not present good agreement with the FAC2 range and slightly high values for VG (although VG values were within the performance criteria proposed by Chang

Table 2
Statistical performance measures for each trial.

Trials	FAC2	FB	NMSE	$MG_{0.1\%}$	$VG_{0.1\%}$	Maximum discrepancy [%]
P1	86	0.2	0.1	1.3	1.2	0.8
P2	94	0.0	0.1	1.0	1.1	1.4
P3	54	0.0	0.3	1.0	2.5	1.8
P4	48	0.1	0.6	1.1	2.2	1.9
P5	90	0.1	0.1	1.1	1.2	1.2
P6	92	0.1	0.1	1.2	1.1	1.6
P7	80	−0.2	0.2	0.8	1.5	1.6
P8	51	0.5	0.4	1.4	1.2	1.2
P9	71	0.2	0.2	1.4	1.8	1.3
P10	72	0.0	0.2	1.3	1.8	0.9
Average over ten trials	74	0.1	0.2	1.2	1.6	–

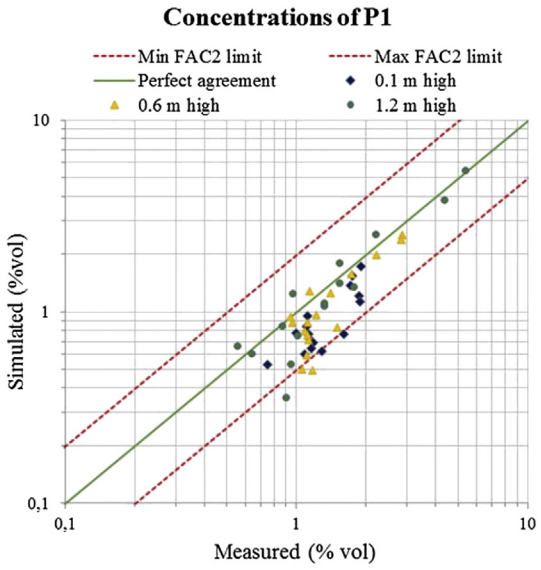

Fig. 6. FAC2 range of trial P1.

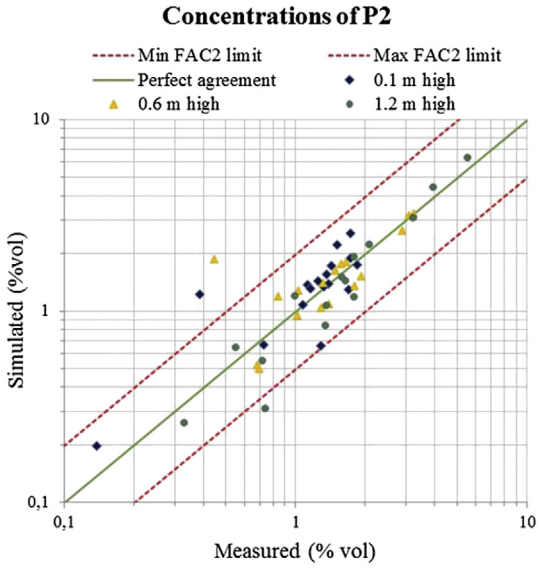

Fig. 7. FAC2 range of trial P2.

and Hanna, 2004), which indicates a significant scatter of the predicted concentrations. As seen in Table 2, 54% and 48% of the predicted peak concentrations of trials P3 and P4, respectively, fell within the FAC2 range (see Figs. 8 and 9).

The same FAC2 analysis was performed considering only the sensors located at the centerline (which is an usual approach to evaluate dispersion models); compared to Figs. 8 and 9, the agreement was greatly enhanced: 85% of the plotted points of trial P3 fell within the FAC2 range and 70% for trial P4. The simulator had larger errors when simulating concentrations out of the dispersion path axis, especially at the higher points.

In order to better understand this issue, the concentration dynamics with time of each monitor point should be analyzed; this analysis shows that the simulated cloud is more sensitive to the wind direction than the actual cloud (the prevailing wind direction during trial P3 and P4 was about 141° and 124°, respectively). This issue can be observed, for example in Fig. 10, comparing the real/simulated concentration evolution over time plotted for three concentration sensors placed 10 m apart from the release point at a height of 1.2 m: the first one, sensor 11C located on the right side of the dispersion path following the jet direction (1 m of displacement in the y direction); the second, sensor 12C, located on the centerline; and the third, sensor 13C, located on the left side (also 1 m displaced). Regarding sensor 12C, placed on the centerline, the measured and predicted concentrations present a very good agreement; however, the other two sensors present poor agreement: the simulator significantly underestimated the values for sensor 13C and overestimated to sensor 11C because the simulated cloud is pushed to the right side by the wind, as shown in Fig. 11.

The simulated cloud was more sensitive to wind effects since a constant wind is considered in the simulations (while carrying out

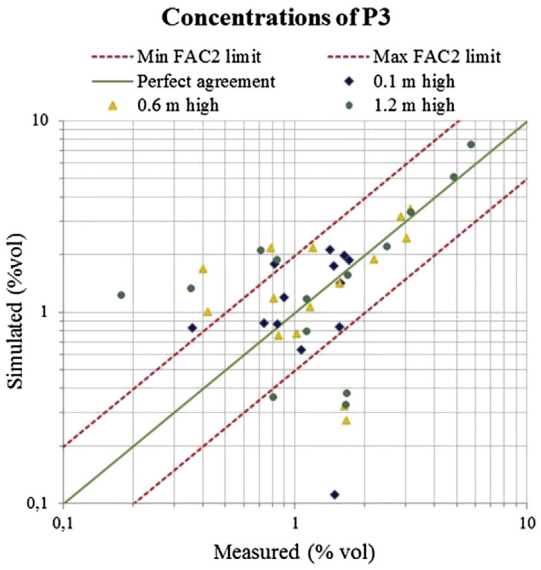

Fig. 8. FAC2 range of trial P3.

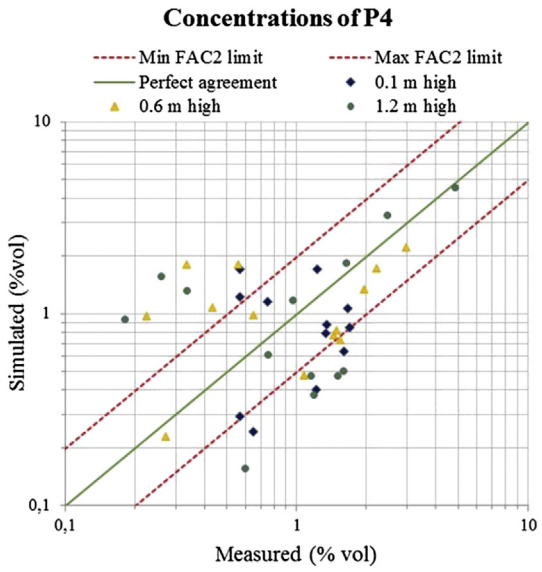

Fig. 9. FAC2 range of trial P4.

Fig. 12, comparing the real/simulated concentration evolution over time plotted for two concentration sensors placed 9 m apart from the release point at a height of 0.6 m: the first one, sensor 9B located on the right side of the dispersion path following the jet direction (2 m of displacement in the y direction); the second, sensor 10B, located on the left side (also displaced 2 m). As in the previous case, the simulator significantly overestimated the values for sensor 9B and underestimated sensor 10B because the simulated cloud is pushed to the right side by the wind, as shown in Fig. 13.

Trials P5, P6 and P7 as well as trials P1 and P2 presented performance measures very close to ideal values (i.e., 88% of the points fall within the FAC2 range); the simulator was able to represent the influence of the fence in the cloud path presenting good accuracy in the whole extension of the cloud path.

Concerning trial P8, 51% of the predicted peak concentrations fall within the FAC2 range, narrowly within the performance criteria presented by Chang and Hanna (2004); Fig. 14 presents the FAC2 range of trial P8; yet the majority of the points that fall without the FAC2 range are not seen in this figure since the predicted concentrations were very close to zero (less than 0.1%). The simulator significantly underestimated the concentrations at the

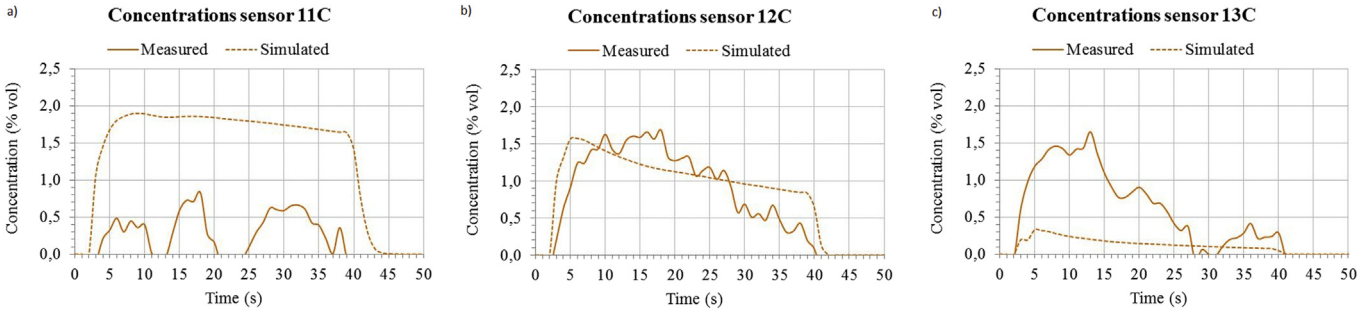

Fig. 10. Measured and simulated concentrations of trial P3 at 10 m from the release point at a 1.2 m height on a) the right side b) the centerline c) the left size of the dispersion path following the jet direction.

trial P3, there were excessive oscillations in wind speed and direction; the wind speed ranged between 0.03 m s^{-1} and 2.97 m s^{-1} and the direction between 16° and 350°), which gives reasonably good results when simulating concentration on the centerline; however, FLACS loses precision when simulating concentrations at a location out of the dispersion path axis.

A similar analysis of trial P4 produced similar conclusions;

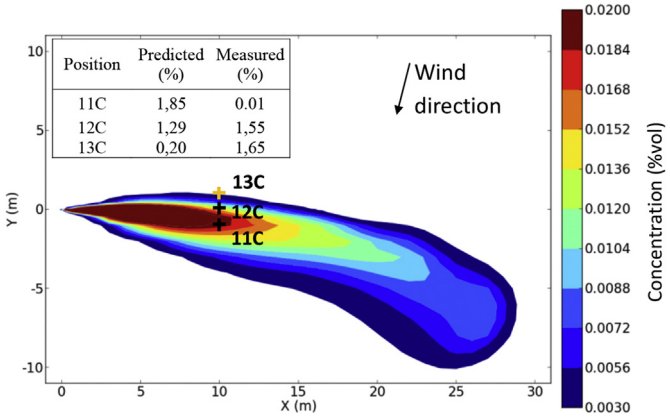

Fig. 11. Cloud profile concentration of Trial P3 at a 1.2 m height, 13 s after the release start.

points located after the barrier, since (as shown in Fig. 15) a large part of the simulated cloud was trapped before the barrier while the actual cloud seems to spread over the barrier. One of the reasons that could explain this particular lack of accuracy could also be found in the simulated wind. A constant wind is considered in the simulation; but along the execution of the test, there were oscillations in wind speed and direction; the wind speed ranged between 0.83 m s^{-1} and 1.67 m s^{-1} and the direction between 161° and 227°. With a simulated wind dynamics simpler than the real one, the simulator may not well represent the spreading of the real cloud during the periods of changes in the wind direction when the actual cloud spreads to the left side of the fence. The effects of wind direction in the jet are important in this layout, since a minor deviation of the jet may trap the cloud or not on one side of the fence. Thus, the results are considerably sensitive to crosswind.

Trials P9 and P10 generally present good agreement between predicted and measured peak concentrations. In trial P9, the simulated cloud was slightly lower than the actual cloud; thus, the simulator moderately underpredicted the peak concentrations at the points far from the release point, since a larger part of the simulated than the actual cloud was trapped before the fence. As in the previous trials, there were oscillations in the wind direction (between 169° and 242°) along the test, which contributed to the cloud spreading; the homogenous wind simulated in the opposite direction of the release did not allow the predicted cloud to spread beyond the fence. Concerning trial P10, the simulator presented

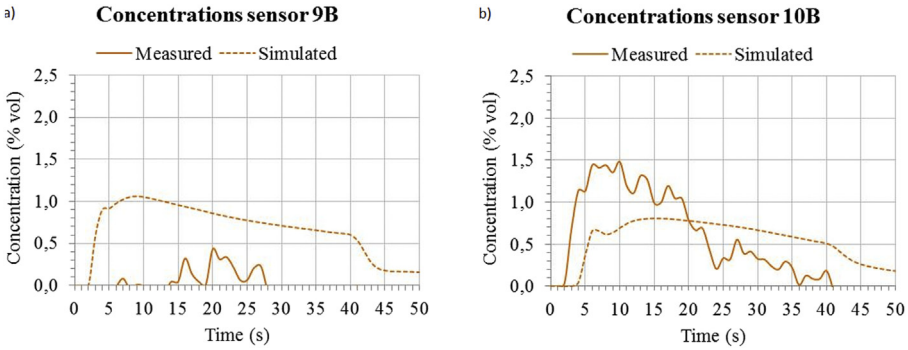

Fig. 12. Measured and simulated concentrations of trial P4 at 9 m from the release point at 0.6 m height a on a) the right side b) the left size of the dispersion path following the jet direction.

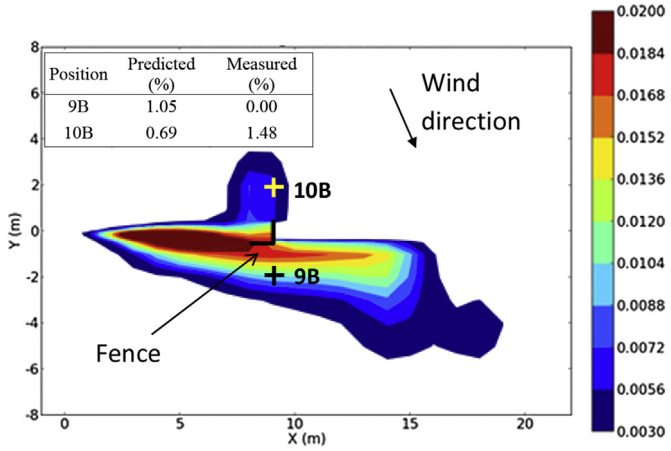

Fig. 13. Cloud profile concentration of Trial P4 at a 0.6-m height, 10 s after the release start.

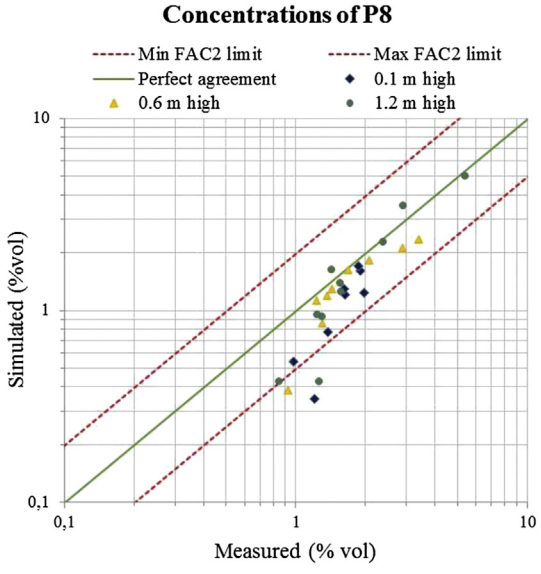

Fig. 14. FAC2 range of trial P8.

good statistical performance measures; there was a very good agreement between the predicted and the measured concentrations for the points located on the centerline (96% of the points fall within the FAC2 range) while the highest discrepancies correspond

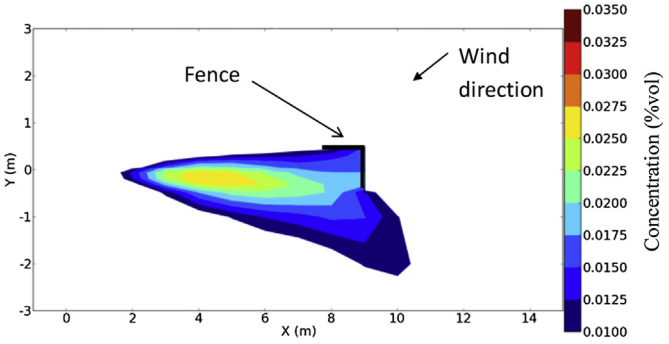

Fig. 15. Cloud profile concentration of Trial P8 at a 0.6 m height, 10 s after the release start.

to the farthest points of the cloud path centerline. As occurred in trials P3 and P4, the simulator had larger errors when simulating concentrations out of the dispersion path axis.

Finally, the last column of Table 2 shows that the divergences between the measured and the predicted peak concentrations are not very high for any trial; the maximum difference occurs in trial P4, in which for the monitor point placed on the centerline 18 m from the release point at a 0.1 m height, the peak concentration measured was equal to 1.9% and the simulation did not predict significant concentrations at this point.

5. Conclusions and future work

This paper presented the field tests performed at USP to provide experimental data about gas dispersion for investigating the performance of CFD tools for cloud dispersion of toxic/flammable substances modeling.

The literature review shows a lack of comprehensive and available experimental data to perform complete validation and comparison studies concerning cloud dispersion; the new experimental data herein will provide insights about the CFD tools performance in dispersion modeling.

The field tests performed at USP consisted of continuous releases of CO_2, consequent cloud formation and dispersion tracking in terms of concentration; the trials were designed to investigate the influence of obstructions placed in the path of the vapor flow; thus, 4 different fences were used for the tests. The data provided are more comprehensive than other published experimental datasets concerning cloud dispersion; the peak concentrations of each sensor (not only for arcs around the release point) and the release rates are provided in the Annex, which will be suitable for the international scientific community interested in

comprehensive models validation and comparison studies, particularly in analysis involving scenarios with obstacles.

The experimental data obtained were compared with CFD simulations in terms of concentrations and typical statistical measures were used to assess the performance of the simulator in dispersion modeling. In general terms, the CFD simulator presented good performance when simulating peak concentrations; all the statistical performance measures (FAC2, FB, MG, NMSE and VG) were well within the acceptable range. It is worth to note that these indicators are well established for dispersion model validation purposes and in the paper at hand were applied using a more rigorous approach in terms of pairing (usually the pairing is made in terms of maximum concentrations measures in concentric arcs at different distances from de release point; here the paring was performed in space for each monitor point). Also noteworthy is that the simulator presented a slight tendency to underestimate the concentrations, but abided by the performance criteria.

The simulator performance also presented sensitivity to wind profile, especially when cross wind occurs; the performance may be improved by setting the scenario considering more complex wind dynamics as the ones encountered during the field tests. CFD simulators consider constant wind profiles for dispersion analysis; however, real scenarios are unlikely to have stable wind. This is certainly an important issue which will be explored in future work.

Acknowledgments

This paper reports part of the overall results from R&D project grant 2013/18218-2 sponsored by the São Paulo Research Foundation (FAPESP), which the authors gratefully wish to acknowledge. The authors also gratefully acknowledge the Program for the Development of Human Resources (PRH19) from Petrobras and the Brazilian National Petroleum, Natural Gas and Biofuels Agency (ANP) for the financial support.

ANNEX A

In this Annex, release rates and peak concentration values of each trial performed during the field tests are presented.

Table A1 shows the discharge rates 1 s-averaged (the duration release of each trial according to Table 1). Tables A2 and A3 present the peak concentrations measured and simulated (in % volume) for each sensor placed in the field tests. The peak concentrations were also 1 s-averaged.

Table A1
Release rates of each trial.

Time	Release rate [kg s^{-1}]									
[s]	P1	P2	P3	P4	P5	P6	P7	P8	P9	P10
1	0.04	0.07	0.09	0.08	0.20	0.38	0.13	0.20	0.14	0.03
2	0.11	0.27	0.52	0.28	0.24	0.38	0.42	0.24	0.49	0.28
3	0.47	0.53	0.72	0.45	0.58	0.57	0.49	0.42	0.61	0.47
4	0.46	0.62	0.80	0.53	0.62	0.58	0.51	0.45	0.63	0.51
5	0.48	0.64	0.83	0.56	0.63	0.58	0.52	0.46	0.63	0.51
6	0.48	0.65	0.84	0.56	0.62	0.58	0.51	0.46	0.63	0.51
7	0.48	0.64	0.84	0.54	0.62	0.57	0.50	0.45	0.62	0.51
8	0.48	0.64	0.83	0.53	0.61	0.57	0.49	0.44	0.62	0.51
9	0.47	0.63	0.83	0.53	0.60	0.56	0.49	0.44	0.62	0.50
10	0.47	0.62	0.82	0.52	0.60	0.56	0.48	0.43	0.61	0.49
11	0.46	0.62	0.81	0.51	0.59	0.54	0.47	0.42	0.61	0.48
12	0.46	0.61	0.80	0.50	0.59	0.53	0.46	0.41	0.60	0.47
13	0.45	0.60	0.79	0.50	0.58	0.53	0.45	0.41	0.60	0.47
14	0.45	0.59	0.79	0.49	0.58	0.52	0.45	0.40	0.60	0.46
15	0.44	0.59	0.78	0.48	0.57	0.51	0.44	0.39	0.59	0.45
16	0.44	0.59	0.77	0.47	0.57	0.51	0.43	0.38	0.59	0.44
17	0.43	0.57	0.77	0.46	0.57	0.50	0.42	0.37	0.58	0.43
18	0.43	0.56	0.76	0.46	0.57	0.50	0.41	0.37	0.58	0.42
19	0.54	0.55	0.75	0.45	0.56	0.49	0.40	0.36	0.58	0.42
20	0.53	0.54	0.74	0.44	0.54	0.48	0.40	0.35	0.57	0.41
21	0.52	0.53	0.74	0.43	0.54	0.48	0.39	0.34	0.57	0.40
22	0.50	0.52	0.73	0.42	0.52	0.47	0.38	0.33	0.56	0.39
23	0.49	0.50	0.72	0.41	0.52	0.46	0.37	0.33	0.56	0.38
24	0.48	0.49	0.72	0.41	0.51	0.46	0.36	0.32	0.54	0.38
25	0.46	0.48	0.71	0.40	0.50	0.45	0.36	0.31	0.53	0.37
26	0.45	0.47	0.70	0.39	0.49	0.44	0.35	0.30	0.53	0.36
27	0.44	0.45	0.70	0.38	0.48	0.44	0.34	0.29	0.52	0.35
28	0.43	0.44	0.69	0.37	0.48	0.43	0.33	0.29	0.51	0.34
29	0.41	0.43	0.68	0.37	0.48	0.43	0.32	0.28	0.50	0.34
30	0.40	0.42	0.68	0.36	0.46	0.42	0.32	0.27	0.50	0.33
31	0.39	0.41	0.67	0.35	0.45	0.41	0.31	0.26	0.49	0.32
32	0.39	0.40	0.67	0.34	0.45	0.41	0.30	0.26	0.49	0.31
33	0.37	0.39	0.66	0.33	–	–	–	0.25	0.48	0.31
34	0.35	0.38	0.66	0.32	–	–	–	0.25	0.47	0.30
35	0.35	0.37	0.65	0.31	–	–	–	0.24	0.46	0.29
36	0.34	0.36	0.64	0.31	–	–	–	0.24	0.46	0.28
37	0.32	0.35	0.64	0.30	–	–	–	0.23	0.45	0.28
38	0.31	0.34	0.63	0.29	–	–	–	0.22	0.45	0.27
39	0.29	0.15	0.63	0.29	–	–	–	0.22	0.44	0.26
40	0.29			0.20	–	–	–	0.20	0.43	0.25
41	–	–	–	–	–	–	–	–	0.42	0.25
42	–	–	–	–	–	–	–	–	0.32	0.24
43	–	–	–	–	–	–	–	–	–	0.24

Table A2
Peak concentrations (trials P1 to P5).

Sensor	P1		P2		P3		P4		P5	
	Measured	Simulated	Measured	Simulated	Measured	Simulated	Measured	Simulated	Measured	Simulated
1A	0.28	0.05	0.14	0.20	0.28	0.08	0.00	0.02	0.15	0.27
1B	1.15	1.29	0.44	1.85	0.40	1.66	0.65	0.97	0.63	1.86
1C	5.35	5.48	5.52	6.39	5.73	7.55	4.83	4.60	6.61	6.38
2A	0.75	0.53	0.39	1.23	0.36	0.83	0.57	0.29	0.35	1.36
2B	2.88	2.52	3.23	3.21	3.14	3.43	2.97	2.19	2.86	3.25
2C	4.33	3.84	3.90	4.46	4.82	5.13	2.46	3.28	4.77	4.44
3A	1.87	1.21	1.52	2.21	1.48	1.74	1.60	0.63	1.45	2.32
3B	2.86	2.38	3.08	3.14	2.87	3.12	2.22	1.70	2.92	3.17
3C	2.18	2.56	3.20	3.09	3.13	3.34	1.63	1.85	3.37	3.07
4A	1.29	0.63	1.29	0.66	1.07	0.64	0.75	1.16	1.05	0.94
4B	1.18	0.49	0.68	0.52	0.42	1.00	0.23	0.97	0.64	0.69
4C	0.90	0.36	0.74	0.31	0.18	1.23	−0.04	0.90	0.31	0.28
5A	1.60	0.76	1.69	1.30	0.82	1.78	1.23	1.70	1.48	1.34
5B	1.14	0.71	1.80	1.33	0.78	2.15	0.56	1.79	0.94	1.27
5C	0.64	0.61	1.35	1.08	0.71	2.11	0.26	1.57	0.85	0.96
6A	1.90	1.73	1.72	2.55	1.63	1.99	1.66	1.06	1.91	2.54
6B	2.24	1.99	2.88	2.61	3.02	2.40	1.95	1.32	2.46	2.64
6C	1.53	1.81	2.08	2.26	2.49	2.21	0.96	1.18	2.65	2.30
7A	1.75	1.54	1.07	1.08	1.12	0.10	1.33	0.79	1.39	1.49
7B	1.75	1.57	1.38	1.08	1.64	0.32	1.54	0.72	1.66	1.45
7C	1.76	1.35	1.34	0.85	1.66	0.38	1.58	0.51	1.32	1.09
8A	1.12	0.95	0.73	0.66	0.82	0.00	1.70	0.85	1.30	0.94
8B	0.97	0.88	0.69	0.49	0.48	0.03	1.44	0.76	0.92	0.76
8C	0.55	0.67	0.33	0.26	0.43	0.04	1.18	0.38	0.67	0.42
9A	1.88	1.13	1.38	1.39	0.84	0.86	0.57	1.22	0.97	0.95
9B	1.52	0.82	1.29	1.03	0.81	1.17	0.43	1.06	0.88	0.74
9C	0.94	0.54	0.55	0.65	0.35	1.35	0.18	0.94	0.42	0.35
10A	1.71	1.37	1.32	1.34	0.81	0.00	1.35	0.87	1.74	1.69
10B	1.42	1.26	1.02	0.94	0.76	0.03	1.48	0.81	1.41	1.34
10C	1.32	1.08	0.72	0.55	0.64	0.05	1.49	0.48	1.15	0.85
11A	1.13	0.76	1.74	1.89	1.41	2.12	0.57	1.71	1.18	0.94
011B	1.09	0.79	1.65	1.78	1.19	2.15	0.33	1.79	1.13	0.71
011C	0.86	0.85	1.64	1.45	0.83	1.90	0.34	1.33	1.16	0.98
12A	1.00	0.77	1.43	1.73	1.70	1.88	0.65	0.24	1.43	1.20
12B	0.95	0.94	1.58	1.75	2.20	1.87	0.27	0.23	1.00	1.06
12C	1.52	1.42	1.78	1.92	1.68	1.57	0.75	0.61	1.97	1.64
13A	1.11	0.84	1.84	1.75	1.48	0.11	1.21	0.40	1.85	1.32
13B	1.13	0.88	1.91	1.51	1.66	0.27	1.07	0.47	1.74	1.45
13C	0.96	1.25	1.77	1.19	1.65	0.33	1.15	0.48	1.71	1.54
14A	1.15	0.72	1.37	1.56	1.58	1.43	0.14	0.10	0.92	0.38
14B	1.22	0.96	1.49	1.61	1.55	1.40	0.24	0.09	1.08	0.65
14C	1.32	1.11	1.57	1.52	1.11	1.18	0.59	0.16	1.53	1.27
15A	1.18	0.69	1.26	1.44	0.90	1.20	−0.13	0.06	1.08	0.30
15B	1.13	0.76	1.32	1.39	1.15	1.06	0.16	0.05	0.97	0.55
15C	1.01	0.76	0.98	1.21	1.12	0.80	0.15	0.04	1.13	0.94
16A	1.16	0.64	1.13	1.37	0.73	0.88	0.43	0.03	1.04	0.47
16B	1.11	0.59	1.02	1.26	1.01	0.77	0.10	0.02	0.83	0.55
017A	1.08	0.60	1.16	1.31	1.56	0.83	1.91	0.00	0.81	0.56
017B	1.06	0.50	0.84	1.19	0.84	0.75	0.30	0.00	0.74	0.58
17C	0.00	0.38	–	–	0.80	0.36	0.27	0.00	1.07	0.64

Table A3
Peak concentrations (trials P6 to P10).

Sensor	P6		P7		P8		P9		P10	
	Measured	Simulated	Measured	Simulated	Measured	Simulated	Measured	Simulated	Measured	Simulated
1A	0.26	0.16	0.24	0.34	0.15	0.05	0.36	0.45	0.32	0.28
1B	1.22	1.73	1.49	1.85	1.37	1.18	1.01	1.75	1.44	1.61
1C	6.51	5.98	6.46	6.50	5.36	5.10	6.83	6.39	5.27	5.41
2A	0.69	1.02	1.24	1.16	0.97	0.54	0.88	1.13	0.98	1.24
2B	4.59	3.00	3.63	3.14	3.40	2.31	2.85	3.18	2.85	2.74
2C	3.94	4.23	2.92	4.54	2.89	3.57	4.35	4.45	3.09	3.90
3A	2.02	1.93	2.01	2.09	1.97	1.24	1.76	2.02	1.53	1.99
3B	3.05	2.90	2.62	3.06	2.89	2.11	3.69	2.94	2.33	2.68
3C	2.87	2.93	2.37	3.14	2.37	2.30	2.90	3.05	2.30	2.73
4A	1.58	0.84	1.06	1.15	1.37	0.77	1.58	1.51	1.00	0.06
4B	0.96	0.66	1.45	0.99	1.30	0.84	1.39	1.49	0.90	0.15
4C	0.50	0.44	1.43	0.53	1.29	0.94	1.06	1.04	0.74	0.16
5A	2.26	1.16	1.25	1.34	1.91	1.61	1.71	1.95	1.35	0.43
5B	2.08	1.09	1.58	1.29	1.68	1.61	1.69	1.95	1.03	0.70
5C	2.01	0.81	1.42	1.05	1.54	1.41	2.09	1.71	0.83	0.69
6A	2.28	2.36	1.89	2.39	1.86	1.71	1.85	2.36	1.54	2.22
6B	2.23	2.45	1.97	2.57	2.07	1.82	2.21	2.48	1.91	2.26
6C	1.69	2.16	1.53	2.31	1.42	1.64	2.00	2.19	1.61	1.97
7A	1.48	1.73	1.43	1.92	1.21	0.35	1.50	1.23	1.21	0.81
7B	1.90	1.50	1.49	1.94	0.92	0.38	1.66	1.22	1.52	0.93
7C	1.84	1.21	1.04	1.59	0.84	0.43	1.60	1.12	1.40	0.85
8A	1.09	0.97	0.57	1.08	0.81	0.09	1.22	1.12	1.09	0.39
8B	1.06	0.71	0.67	1.18	0.43	0.09	1.32	1.08	0.95	0.41
8C	1.15	0.47	0.63	1.03	0.35	0.05	0.77	0.99	0.98	0.40
9A	1.78	1.56	1.09	1.05	1.64	1.22	1.84	1.41	1.03	0.10
9B	1.79	1.15	1.20	0.77	1.22	1.11	1.41	1.44	0.85	0.19
9C	1.00	0.85	1.20	0.41	1.23	0.96	1.24	1.31	0.61	0.19
10A	1.20	1.12	1.21	1.64	0.83	0.00	1.92	1.33	1.22	0.47
10B	1.39	0.69	0.93	1.43	0.69	0.00	1.35	1.15	1.08	0.48
10C	1.31	0.54	0.95	1.09	0.68	0.02	0.96	0.97	0.95	0.45
11A	2.29	1.79	0.91	0.63	1.61	1.29	1.28	0.28	1.01	0.72
11B	2.05	1.65	1.05	0.54	1.43	1.28	1.10	0.38	1.20	0.81
11C	1.85	1.37	1.18	0.73	1.55	1.26	1.78	0.98	1.14	0.72
12A	1.78	1.89	0.60	0.53	1.07	0.01	1.30	0.16	1.46	2.12
12B	1.71	1.76	0.71	0.78	0.95	0.01	1.12	0.24	1.23	1.89
12C	2.03	1.87	0.98	1.37	1.25	0.43	1.44	1.10	1.04	1.50
13A	1.64	1.61	0.58	1.66	1.23	0.00	1.63	0.40	1.29	1.04
13B	1.60	1.20	0.74	1.62	0.54	0.00	1.30	0.51	1.05	1.04
13C	1.47	1.24	1.03	1.49	0.87	0.04	1.57	0.85	1.30	0.89
14A	1.40	1.64	0.95	0.98	0.94	0.03	1.39	0.12	1.41	1.96
14B	1.54	1.47	0.72	0.81	0.95	0.03	1.49	0.31	1.20	1.62
14C	1.60	1.58	0.97	0.74	1.03	0.04	1.19	0.66	0.71	1.21
15A	1.25	1.26	0.44	1.12	1.02	0.02	1.39	0.08	1.07	1.79
15B	1.29	1.28	0.29	1.02	0.75	0.02	0.70	0.24	0.83	1.42
15C	1.16	1.34	0.30	0.85	0.75	0.02	0.95	0.54	0.88	1.03
16A	1.03	1.04	0.13	0.80	0.69	0.00	1.06	0.05	0.79	1.64
16B	1.03	1.13	0.09	0.80	0.88	0.00	1.18	0.10	0.94	1.27
17A	1.16	0.98	0.13	0.19	0.95	0.00	0.85	0.01	0.97	1.51
17B	1.05	1.02	0.07	0.27	0.66	0.00	1.04	0.04	0.89	1.16
17C	1.12	1.03	0.16	0.32	0.80	0.00	0.85	0.09	0.69	0.82

References

Albani, R.A., Duda, F.P., Pimentel, L.G., 2015. On the modeling of atmospheric pollutant dispersion during a diurnal cycle: a finite element study. Atmos. Environ. 118, 19–27.

Chang, J.C., Hanna, S.R., 2004. Air quality model performance evaluation. Meteorology Atmos. Phys. 87, 167–196.

City Technology Limited, 5 de January de 2010. OP02-Electrochemical Capillary Controlled Oxygen Sensors (Hampshire, UK).

Coldrick, S., Lea, C.J., Ivings, M.J., 2009. Validation Database for Evaluating Vapor Dispersion Model for Safety Analysis of LNG Facilities – Review. The fire protection research foundation.

Cormier, B.R., Ruifeng, Q., Yun, G., Zhang, Y., Mannan, M.S., 2009. Application of computational fluid dynamics for LNG vapor dispersion modeling: a study of key parameters. J. Loss Prev. Process Industries 332–352.

Gant, S.E., Kelsey, A., McNally, K., Witlox, H., Biblio, M., 2013. Sensitivity analysis of dispersion models for jet releases of dense-phase carbon dioxide. Chem. Eng. Trans. 31, 1–6.

GexCon, A.S., 2013a. FLACS Software: Version 10.3.

GexCon, A.S., 2013b. FLACS v10.0 User's Manual (Norway).

Hanna, S.R., Hansen, O.R., Dharmavaram, S., 2004. FLACS CFD air quality model performance evaluation with Kit Fox, MUST, Praire Grass, and EMU observations. Atmos. Enviroment 38, 4675–4687.

Ivings, M.J., Lea, C.J., Lea, C.J., Webber, D.M., 2007. Evaluating Vapor Dispersion Models for Safety Analysis of LNG Facilities. The fire protection research foundation.

Ivings, M.J., Lea, C.J., Webber, D.M., Jagger, S.F., Coldrick, S., 2013. A protocol for the evaluation of LNG vapour dispersion models. J. Loss Prev. Process Industries 26, 153–163.

Kumar, P., Feiz, A.-A., Ngae, P., Singh, S., Issartel, J.P., 2015. CFD simulation of short-range plume dispersion from a point release in an urban like environment. Atmos. Environ.

Liu, X., Godbole, A., Lu, C., Michal, G., Venton, P., 2015. Study of the consequences of CO2 released from high-pressures pipelines. Atmos. Environ. 116, 51–64.

Mazzoldi, A., Hill, T., Colls, J.J., 2008. CFD and Gaussian atmospheric dispersion models: a comparison for leak. Atmos. Environ. 42, 8046–8054.

Pandya, N., Gabas, N., Marsden, E., 2012. Sensitivity analysis of Phast's atmospheric dispersion model for three toxic materials (nitric oxide, ammonia, chlorine). J. Loss Prev. Process Industries 25, 20–32.

Plasmans, J., Donnat, L., de Carvalho, E., Debelle, T., 2012. Challenges with the use of CFD for major accident dispersion modeling. Process Saf. Prog. 32, 1–8.

Schleder, A.M., Martins, M.R., Pastor, E., Planas, E., 2014a. The Effect of the Computational Grid Size on the Prediction of a Flammable Cloud Dispersion.

Proceedings of the ASME 2014 33th International Conference on Ocean, Offshore and Arctic Engineering - OMAE2014, pp. 1–9 (San Francisco).
Schleder, A.M., Martins, M.R., Pastor, E., Planas, E., 2014b. The Effect of the Environment Conditions on the Prediction of Flammable Cloud Dispersion. Proceedings of European Safety and Reliability Conference - ESREL2014, pp. 1–8 (Wroclaw).
Schleder, A.M., Pastor, E., Planas, E., Martins, M.R., 2015. Experimental data and CFD performance for cloud dispersion analysis: the USP-UPC project. J. Loss Prev. Process Industries 38, 125–138.
Sklavounos, S., Rigas, F., 2006. Simulation of Coyote series trials—Part I: CFD estimation of non-isothermal LNG releases and comparison with box-model predictions. Chem. Eng. Sci. 61, 1434–1443.
Tauseef, S.M., Rashtchian, D., Abbasi, S.A., 2011. CFD-based simulation of dense gas dispersion in presence of obstacles. J. Loss Prev. Process Industries 24, 371–376.
Weil, J.C., Sykes, R.I., Venkatram, A., 1992. Evaluating air-quality models: review and outlook. J. Appl. Meterorology 31, 1121–1145.
Xing, J., Zhenyi, L., Huang, P., Feng, C., Sun, R., Wang, S., 2014. CFD validation of scaling rules for reduced-scale field releases. Appl. Energy 115, 525–530.